Iterative procedure for multidimensional Euler equations

W. Dreyer, M. Kunik, K. Sabelfeld,
N. Simonov*, and K. Wilmanski

Weierstraß Institute for Applied Analysis and Stochastics
Mohrenstraße 39, 10117 Berlin, Germany
E-mails: dreyer@wias-berlin.de, kunik@wias-berlin.de
sabelfel@wias-berlin.de, wilmanski@wias-berlin.de

* Institute of Computational Mathem. and Mathem. Geophysics
Siberian Branch of Russian Academy of Sciences,
Lavrentiev str., 6, 630090, Novosibirsk, Russia
E-mail: nas@osmf.sscc.ru

Abstracts — A numerical iterative scheme is suggested to solve the Euler equations in two and three dimensions. The step of the iteration procedure consists of integration over the velocity which is here carried out by three different approximate integration methods, and in particular, by a special Monte Carlo technique. Regarding the Monte Carlo integration, we suggest a dependent sampling technique which ensures that the statistical errors are quite small and uniform in space and time. Comparisons of the Monte Carlo calculations with the trapezoidal rule and a gaussian integration method show good agreement.

1 Introduction

We consider a monatomic ideal gas and describe its thermodynamic state by the fields of mass density $\rho(t,\mathbf{x})$, momentum density $(\rho v_i)(t,\mathbf{x})$ and temperature $T(t,\mathbf{x})$, depending on time $t \geq 0$ and space $\mathbf{x} \in \mathbb{R}^3$:

$$\begin{aligned} &\frac{\partial \rho}{\partial t} + \frac{\partial(\rho v_k)}{\partial x_k} = 0 \ , \\ &\frac{\partial(\rho v_i)}{\partial t} + \frac{\partial(\rho v_i v_k + \rho T \delta_{ik})}{\partial x_k} = 0 \ , \\ &\frac{\partial(\rho \frac{v^2}{2} + \frac{3}{2}\rho T)}{\partial t} + \frac{\partial\left(\rho v_k \left(\frac{v^2}{2} + \frac{5}{2} T\right)\right)}{\partial x_k} = 0 \ . \end{aligned} \tag{1.1}$$

These equations constitute the conservation of mass, momentum and energy. At the initial time $t = 0$ we prescribe bounded and integrable initial data for $x \in \mathbb{R}^3$:

$$\rho(0,\mathbf{x}) = \rho_0(\mathbf{x}) \geq \delta > 0, \quad \mathbf{v}(0,\mathbf{x}) = \mathbf{v}_0(\mathbf{x}), \quad T(0,\mathbf{x}) = t_0(\mathbf{x}) \geq \delta' > 0. \tag{1.2}$$

It is well known that in general the initial value problem (1.1) – (1.2) leads to shock-discontinuities. Therefore we need the conservation laws in its original integral form, which takes discontinuities into account. To this end we choose the five field variable u_A and the corresponding fluxes

F_{Ak} $(A = 0, 1, 2, 3, 4; k = 1, 2, 3)$ according to

$$u_A = \begin{pmatrix} \rho \\ \rho \mathbf{v} \\ \rho \frac{v^2}{2} + \frac{3}{2} \rho T \end{pmatrix}, \qquad F_{Ak} = \begin{pmatrix} \rho v_k \\ \rho \mathbf{f} \\ \rho v_k \left(\frac{v^2}{2} + \frac{5}{2} T \right) \end{pmatrix}, \tag{1.3}$$

where the column-vector $\mathbf{f}$ has its components $f_i = v_i v_k + T \delta_{ik}$, $i = 1, 2, 3$.

We define also the entropy density and entropy flux by

$$h = \frac{3}{2} \rho \ln \left(T \rho^{-\frac{3}{2}} \right), \qquad \Phi_k = h v_k. \tag{1.4}$$

Let $\Omega \subset \mathbb{R}^3 \times \mathbb{R}_0^+$ be any bounded convex region in space and time. By $d\vec{o}$ we denote a positive oriented boundary element of $\partial\Omega$. We are now looking for a weak solution $\rho, \mathbf{v}, T$ which satisfies

- the initial data (1.2),
- the conservation laws

$$\int_{\partial\Omega} (u_A, F_{Ak}) \, d\vec{o} \; = \; 0, \tag{1.5}$$

- the entropy inequality

$$\int_{\partial\Omega} (h, \Phi_k) \, d\vec{o} \; \geq \; 0. \tag{1.6}$$

The brackets (u_A, F_{Ak}) and (h, Φ_k) are four-vectors in time (first position) and space (second position). Note that in regular points $(t, \mathbf{x})$ the Gaussian Divergence Theorem applied to (1.5) and (1.6) leads to

$$\frac{\partial u_A}{\partial t} + \frac{\partial F_{Ak}}{\partial x_k} = 0 \tag{1.7}$$

$$\frac{\partial h}{\partial t} + \frac{\partial \Phi_k}{\partial x_k} = 0. \tag{1.8}$$

(1.7) abbreviates (1.1), and the additional conservation law (1.8) give rise to the notion "isentropic" Euler equations. Note that this is misleading, since entropy is produced across the shock fronts.
The weak solution of the initial value problem can be obtained by the following scheme, which is described in [3] in great detail:

To initiate the scheme we start with:

- Bounded and integrable initial data for $x \in \mathbb{R}^3$ as in (1.2).
- A fixed time $\varepsilon > 0$, which gives the equidistant times $t_n = n \cdot \varepsilon$, $n = 0, 1, 2, \ldots$.

The following scheme defines ε-dependent fields $u_A^\varepsilon(t, \mathbf{x})$ and ε-dependent fluxes $F_{Ak}^\varepsilon(t, \mathbf{x})$ for all times $t \geq 0$, where $0 < \tau \leq \varepsilon$, $A = 0, 1, 2, 3, 4$, $k = 1, 2, 3$:

$$\left.\begin{aligned} u_A^\varepsilon(t_n + \tau, \mathbf{x}) &= \int_{-\infty}^{+\infty} c_A f_n^{(3D)}(\mathbf{x} - \tau\mathbf{c}, \mathbf{c})\, d^3\mathbf{c} \\ F_{Ak}^\varepsilon(t_n + \tau, \mathbf{x}) &= \int_{-\infty}^{+\infty} c_A c_k f_n^{(3D)}(\mathbf{x} - \tau\mathbf{c}, \mathbf{c})\, d^3\mathbf{c} \end{aligned}\right\}. \tag{1.9}$$

Here $f_n^{(3D)}$ is the three-dimensional Maxwellian phase density

$$f_n^{(3D)}(\mathbf{y}, \mathbf{c}) = \frac{\rho(t_n, \mathbf{y})}{(2\pi T(_n, \mathbf{y}))^{3/2}} \cdot \exp\left(- \frac{(\mathbf{c} - \mathbf{v}(t_n, \mathbf{y}))^2}{2T(t_n, \mathbf{y})} \right), \tag{1.10}$$

and c_A abbreviates

$$c_A = \begin{cases} 1, & A = 0 \\ c_i, & A = i = 1, 2, 3 \\ \frac{1}{2}|c|^2, & A = 4. \end{cases} \tag{1.11}$$

The ε-dependent entropy-density and entropy flux are

$$\left.\begin{aligned} h^\varepsilon(t_n + \tau, \mathbf{x}) &= -\int_{-\infty}^{+\infty} (f_n^{(3D)} \ln f_n^{(3D)})(\mathbf{x} - \tau\mathbf{c}, \mathbf{c})\, d^3\mathbf{c} \\ \Phi_K^\varepsilon(t_n + \tau, \mathbf{x}) &= -\int_{-\infty}^{+\infty} c_k (f_n^{(3D)} \ln f_n^{(3D)})(\mathbf{x} - \tau\mathbf{c}, \mathbf{c})\, d^3\mathbf{c} \end{aligned}\right\}. \tag{1.12}$$

Remark In contrast to the quantities u_A, F_{Ak}, h, Φ_k given by (1.3) and (1.4), which depend locally on ρ, v_i, T, the ε-dependent fields $u_A^\varepsilon, F_{Ak}^\varepsilon, h^\varepsilon, \Phi_k^\varepsilon$ do not depend locally on

$$\begin{aligned} \rho^\varepsilon &:= u_0^\varepsilon \\ v_i^\varepsilon &:= u_i^\varepsilon / \rho^\varepsilon \quad (i = 1, 2, 3) \\ T^\varepsilon &:= \frac{2}{3}\left(u_4^\varepsilon / \rho^\varepsilon - \frac{1}{2} \left| \mathbf{v}^\varepsilon \right|^2 \right). \end{aligned} \tag{1.13}$$

The fields (1.13) at time $t_n + \tau$ and position $\mathbf{x}$ depend on the global fields $u_A(t_n, \cdot)$ at time t_n.

Next we formulate the main properties of this scheme, which are taken from [3]:

Proposition 1 *Let $\Omega \subset \mathbb{R}^3 \times \mathbb{R}_0^+$ be any bounded convex region in space and time. As before, $d\vec{o}$ denotes a positive oriented boundary element of $\partial\Omega$.*

(i) The representations (1.9) satisfy the conservation laws:

$$\int\limits_{\partial\Omega} (u_A^\varepsilon, F_{Ak}^\varepsilon)\, d\vec{o} \;=\; 0, \qquad A = 0, \ldots, 4.$$

(ii) The representations (1.12) satisfy the entropy inequality:

$$\int\limits_{\partial\Omega} (h_A^\varepsilon, \Phi_k^\varepsilon)\, d\vec{o} \;\geq\; 0.$$

(iii) Let $t > 0$ be fixed. If there exists the L_1-limit of $u_A^\varepsilon(t_n, \cdot)$ for $\varepsilon \to 0$, then

$$u_A^\varepsilon \underset{L_1}{\longrightarrow} u_A, \qquad F_{Ak}^\varepsilon \underset{L_1}{\longrightarrow} F_{Ak},$$

$$h^\varepsilon \underset{L_1}{\longrightarrow} h, \qquad \Phi_k^\varepsilon \underset{L_1}{\longrightarrow} \Phi_k,$$

where the Eulerian limits u_A, F_{Ak}, h, Φ_k of (1.9) and (1.12) satisfy the algebraic conditions (1.3) and (1.4).

In the following we consider exclusively the case $\varepsilon > 0$. Therefore we shall omit the index ε in all ε-dependent fields. This will not lead to confusions. For numerical purposes we mostly consider the two-dimensional case, which will be evaluated now.

We are looking for solutions $u_A(t, x_1, x_2, x_3)$ which do not depend on x_3. In this case we can carry out the c_3-integration in (1.9) and obtain the two-dimensional scheme for $\rho, \mathbf{v} = (v_1, v_2)$ and T:

$$\begin{aligned}
\rho(t_n + \tau, \mathbf{x}) &= \int_{-\infty}^{+\infty} f_n(\mathbf{x} - \tau\mathbf{c}, \mathbf{c})\, d^2\mathbf{c}, \\
(\rho v_i)(t_n + \tau, \mathbf{x}) &= \int_{-\infty}^{+\infty} c_i f_n(\mathbf{x} - \tau\mathbf{c}, \mathbf{c})\, d^2\mathbf{c}, \qquad (1.14) \\
\left(\rho\frac{v^2}{2} + \frac{3}{2}\rho T\right)(t_n + \tau, \mathbf{x}) &= \int_{-\infty}^{+\infty} \left(\frac{c^2}{2} + \frac{1}{2}T(t_n, \mathbf{x} - \tau\mathbf{c})\right) f_n(\mathbf{x} - \tau\mathbf{c}, \mathbf{c})\, d^2\mathbf{c}.
\end{aligned}$$

Here $\mathbf{x}, \mathbf{c}, \mathbf{v} \in \mathbb{R}^2$, $i = 1, 2$, and $f_n = f_n(\mathbf{y}, \mathbf{c})$ is the two-dimensional Maxwellian density

$$f_n(\mathbf{y}, \mathbf{c}) = \frac{\rho(t_n, \mathbf{y})}{2\pi T(t_n, \mathbf{y})} \cdot \exp\left[-\frac{(\mathbf{c} - \mathbf{v}(t_n, \mathbf{y}))^2}{2T(t_n, \mathbf{y})}\right]. \qquad (1.15)$$

Note that the temperature appears now also on the right hand side in the last equation of (1.14). It is important to realize that the two-dimensional representations (1.14) result from the microscopically three-dimensional model (1.9).

The scheme (1.14) requires initial data $\rho(0, \mathbf{x}) = \rho_0(\mathbf{x})$, $\mathbf{v}(0, \mathbf{x}) = v_0(\mathbf{x})$ and $T(0, \mathbf{x}) = T_0(\mathbf{x})$ which only depend on $\mathbf{x} \in \mathbb{R}^2$. Next we will evaluate the integrals (1.14). To this purpose we will use deterministic as well as Monte-Carlo methods. The comparison of these methods is the main objective of this paper.
It is sometimes useful to introduce the integral substitution $\mathbf{y} = \mathbf{x} - \tau\mathbf{c}$ which transforms (1.14) into

$$\rho(t_n+\tau,\mathbf{x}) = \frac{1}{\tau^2}\int\limits_{-\infty}^{+\infty} f_n(\mathbf{y},\frac{1}{\tau}(\mathbf{x}-\mathbf{y}))\,d^2\mathbf{y}$$

$$(\rho v_i)(t_n+\tau,\mathbf{x}) = \frac{1}{\tau^2}\int\limits_{-\infty}^{+\infty} \frac{x_i-y_i}{\tau}\, f_n(\mathbf{y},\frac{1}{\tau}(\mathbf{x}-\mathbf{y}))\,d^2\mathbf{y}, \quad (1.16)$$

$$\left(\rho\frac{v^2}{2}+\frac{3}{2}\rho T\right)(t_n+\tau,\mathbf{x}) = \frac{1}{\tau^2}\int\limits_{-\infty}^{+\infty}\left[\frac{1}{2\tau}(\mathbf{x}-\mathbf{y})^2+\frac{1}{2}T(t_n,\mathbf{y})\right] \times f_n(\mathbf{y},\frac{1}{\tau}(\mathbf{x}-\mathbf{y}))\,d^2\mathbf{y}.$$

2 Deterministic integration method, Part I : The trapezoidal rule

In this section we apply the trapezoidal rule to the integral representations (1.14). At the beginning we need a sufficiently large rectangular domain

$$\mathcal{R} = \left[c_1^{\min}, c_1^{\max}\right] \times \left[c_2^{\min}, c_2^{\max}\right] \quad (2.1)$$

so that the Maxwellian $f_n(\mathbf{y},\mathbf{c})$ in (1.15) is sufficiently small outside of $\mathcal{R}$. In order to construct $\mathcal{R}$, we use the knowledge of the dynamic fields at the preceeding time step t_n. Thus at the actual time t_{n+1}, the size of $\mathcal{R}$ is determined as follows:

We choose $\mathcal{R}$ and a positive constant $\gamma \geq 3$, for example $\gamma = 4$, so that each $\mathbf{c}$ which is outside of $\mathcal{R}$ must satisfy the inequality (2.2) for all $\mathbf{y} \in \mathbb{R}^2$:

$$\exp\left[-\frac{(\mathbf{c}-\mathbf{v}(t_n,\mathbf{y}))^2}{2T(t_n,\mathbf{y})}\right] < \exp\left(-\gamma^2\right) = \exp\left(-16\right) = 1,125\cdot 10^{-7}. \quad (2.2)$$

We are able to control the following extreme values of the fields $\mathbf{v}(t_n,\cdot)$ and

$T(t_n, \cdot)$ at the previous time step t_n:

$$\left.\begin{aligned} v_1^{\min} &= \min_{\mathbf{y}\in\mathbb{R}^2} v_1(t_n,\mathbf{y}), \quad v_1^{\max} = \max_{\mathbf{y}\in\mathbb{R}^2} v_1(t_n,\mathbf{y}), \\ v_2^{\min} &= \min_{\mathbf{y}\in\mathbb{R}^2} v_2(t_n,\mathbf{y}), \quad v_2^{\max} = \max_{\mathbf{y}\in\mathbb{R}^2} v_2(t_n,\mathbf{y}), \\ T^{\min} &= \min_{\mathbf{y}\in\mathbb{R}^2} T(t_n,\mathbf{y}), \quad T^{\max} = \max_{\mathbf{y}\in\mathbb{R}^2} T(t_n,\mathbf{y}). \end{aligned}\right\} \tag{2.3}$$

Consequently it is an easy matter to examine that an appropriate choice of the integration domain $\mathcal{R}$ is given by the following square with the side length r :

$$\left.\begin{aligned} r &= \frac{1}{2}\left[\left(v_1^{\min}-v_1^{\max}\right)^2+\left(v_2^{\min}-v_2^{\max}\right)^2\right]^{1/2}+\gamma\sqrt{2T^{\max}}, \\ c_1^{\min} &= \frac{1}{2}\left(v_1^{\min}+v_1^{\max}\right)-r\ , \quad c_1^{\max} = \frac{1}{2}\left(v_1^{\min}+v_1^{\max}\right)+r, \\ c_2^{\min} &= \frac{1}{2}\left(v_2^{\min}+v_2^{\max}\right)-r\ , \quad c_2^{\max} = \frac{1}{2}\left(v_2^{\min}+v_2^{\max}\right)+r. \end{aligned}\right\} \tag{2.4}$$

Finally we have to solve the problem of space-discretization. To this end we choose a rectangular and static $\Omega \subset \mathbb{R}^2$ according to the following procedure:

We start with initial data $\rho_0, \mathbf{v}_0, T_0$, which assume constant values $\hat{\rho}_0, \hat{\mathbf{v}}_0, \hat{T}_0$ corresponding to an equilibrium state outside some bounded region $\hat{\Omega} \subset \mathbb{R}^2$. Then we choose $\Omega \supset \hat{\Omega}$ large enough so that within a finite time interval $0 \le t \le t_{fin}$ the solution still assumes the constant values $\hat{\rho}_0, \hat{\mathbf{v}}_0$, $\hat{T}_0$ up to a relative error $|1-\frac{\rho}{\hat{\rho}_0}| \le \delta \ll 1$ on the boundary $\partial\Omega$ of Ω. If that condition is satisfied we set the fields $\rho(t_n,\mathbf{y})$, $\mathbf{v}(t_n,\mathbf{y})$, $T(t_n,\mathbf{y})$ equal to the constant values $\hat{\rho}_0$, $\hat{\mathbf{v}}_0$, $\hat{T}_0$ whenever $\mathbf{y}$ is outside Ω and $0 \le t_n \le t_{fin}$.

Although Ω depends on the initial data and on the final t_{fin}, it does not constitute a dynamic domain. Ω must be nevertheless enlarged with t_{fin} according to the speeds of travelling (shock-) waves.

Next we cover the resulting domain

$$\Omega = \left[x_1^{\min}\,,\, x_1^{\max}\right] \times \left[x_2^{\min}\,,\, x_2^{\max}\right] \tag{2.5}$$

with a rectangular mesh with meshpoints

$$x_1^{(i)} := x_1^{\min} + i\,\frac{x_1^{\max} - x_1^{\min}}{n_1 - 1}, \qquad x_2^{(j)} := x_2^{\min} + j\,\frac{x_2^{\max} - x_2^{\min}}{n_2 - 1},$$

where $0 \le i < n_1$, $0 \le j < n_2$ and $n_1, n_2 \ge 2$ are the numbers of grid points in the x_1 and x_2 direction, respectively. Then we decompose each rectangle $\left[x_1^{(i)}, x_1^{(i+1)}\right] \times \left[x_2^{(j)}, x_2^{(j+1)}\right]$ into two triangles so that the final decomposition of Ω is as follows:

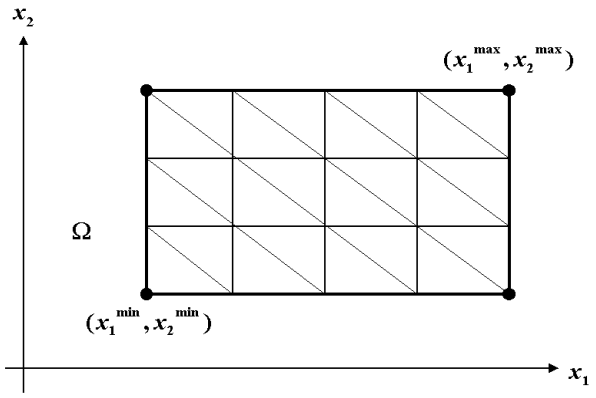

Figure 1: Decomposition of Ω.

The new fields $\rho(t_{n+1}, \cdot), \mathbf{v}(t_{n+1}, \cdot)$, $T(t_{n+1}, \cdot)$ are computed at the grid points $x_1^{(i)}, x_2^{(j)}$ relying on the knowledge of the previous fields, which are interpolated linearly to each triangle. The linear interpolation of the previous fields corresponds to the application of the trapezoidal integration rule in (1.14) to each triangle.

3 Deterministic integration method, Part II: A Gaussian integration rule

The trapezoidal integration method which we proposed in the last section leads to three disadvantages: The number of **c**-integration points must be large enough in order to keep the scheme stable, the integration domain changes in each new time step, and moreover this integration method does not take into account explicitely the appearence of Gaussian factors in the

integrals (1.14) for very small values of τ: Assume that at some point $\mathbf{x} \in \mathbb{R}^2$ the fields $\rho(t_n, \mathbf{x})$, $\mathbf{v}(t_n, \mathbf{x})$, $T(t_n, \mathbf{x})$ do not change very much in space and that $\tau \ll 1$. Then the $\mathbf{c}$-dependent fields $\rho(t_n, \mathbf{x} - \tau\mathbf{c})$, $\mathbf{v}(t_n, \mathbf{x} - \tau\mathbf{c})$ and $T(t_n, \mathbf{x} - \tau\mathbf{c})$ also do not change very much (for fixed $t_n, \mathbf{x}$) within a finite $\mathbf{c}$-region. In this case $f_n(\mathbf{x} - \tau\mathbf{c}, \mathbf{c})$ agrees approximately with the Gaussian kernel $f_n(\mathbf{x}, \mathbf{c})$.

Therefore we introduce the following functions of $\mathbf{c}$, which depend on the fixed parameters $t_n, \tau, \mathbf{x}$:

$$\begin{aligned} \varphi_\rho(t_n, \tau, \mathbf{x}; \mathbf{c}) &= \frac{f_n(\mathbf{x} - \tau\mathbf{c}, \mathbf{c})}{f_n(\mathbf{x}, \mathbf{c})}, \\ \varphi_{v_i}(t_n, \tau, \mathbf{x}; \mathbf{c}) &= c_i \, \frac{f_n(\mathbf{x} - \tau\mathbf{c}, \mathbf{c})}{f_n(\mathbf{x}, \mathbf{c})}, \\ \varphi_T(t_n, \tau, \mathbf{x}; \mathbf{c}) &= \left(\frac{c^2}{2} + \frac{1}{2} T(t_n, \mathbf{x} - \tau\mathbf{c}) \right) \frac{f_n(\mathbf{x} - \tau\mathbf{c}, \mathbf{c})}{f_n(\mathbf{x}, \mathbf{c})}. \end{aligned} \tag{3.1}$$

We have to integrate these φ-functions with respect to the Gaussian kernel $f_n(\mathbf{x}, \mathbf{c})$:

$$\left.\begin{aligned} \rho(t_n + \tau, \mathbf{x}) &= \int_{-\infty}^{+\infty} \varphi_\rho(t_n, \tau, \mathbf{x}; \mathbf{c}) f_n(\mathbf{x}, \mathbf{c}) \, d^2\mathbf{c} \ , \\ (\rho v_i)(t_n + \tau, \mathbf{x}) &= \int_{-\infty}^{+\infty} \varphi_{v_i}(t_n, \tau, \mathbf{x}; \mathbf{c}) f_n(\mathbf{x}, \mathbf{c}) \, d^2\mathbf{c} \ , \\ \left(\rho\tfrac{v^2}{2} + \tfrac{3}{2}\rho T \right)(t_n + \tau, \mathbf{x}) &= \int_{-\infty}^{+\infty} \varphi_T(t_n, \tau, \mathbf{x}; \mathbf{c}) f_n(\mathbf{x}, \mathbf{c}) \, d^2\mathbf{c}. \end{aligned}\right\} \tag{3.2}$$

The integrals (3.2) were evaluated approximately by A.-H. Stroud and Don Secrest in [8]. In the two-dimensional case their formulas may be written in the form

$$\frac{1}{2\pi} \int_{-\infty}^{+\infty} \varphi(c_1, c_2) \cdot e^{-\frac{c_1^2 + c_2^2}{2}} dc_1 dc_2 = \sum_{i=1}^{N} A_i f\left(c_1^{(i)}, c_2^{(i)} \right), \tag{3.3}$$

where A_i are constants and $P_i = \left(c_1^{(i)}, c_2^{(i)}\right)$ denote the integration knodes. If ϕ were a polynomial of maximal degree k, then one can choose the k-dependent quantities A_i and the integration knodes P_i so that (3.3) is exactly satisfied. Here the functions ϕ_ρ, ϕ_{v_i} and ϕ_T are not polynomials, and the equation (3.3) is satisfied approximately. In the following we choose $k = 7$, i.e. the equation (3.3) may be evaluated with only 12 integration knodes exactly for each polynomial ϕ of maximal degree 7. Let

$$\begin{aligned} &\nu = \sqrt{6}, \quad \xi = \frac{1}{2}\sqrt{9 - 3\sqrt{5}}, \quad \eta = \frac{1}{2}\sqrt{9 + 3\sqrt{5}}, \\ &A = \frac{1}{36}, \qquad b = \frac{5 + 2\sqrt{5}}{45}, \qquad c = \frac{5 - 2\sqrt{5}}{45}. \end{aligned} \tag{3.4}$$

Explicitly we obtain for each polynomial φ with degree ≤ 7:

$$\begin{aligned} &\frac{1}{2\pi}\int_{-\infty}^{+\infty} \varphi(c_1, c_2) e^{-\frac{c_1^2 + c_2^2}{2}} dc_1 dc_2 \qquad (3.5) \\ &\qquad = A \cdot \Big[\varphi(\nu, 0) + \varphi(-\nu, 0) + \varphi(0, \nu) + \varphi(0, -\nu)\Big] \\ &\qquad +B \cdot \Big[\varphi(\xi, \xi) + \varphi(\xi, -\xi) + \varphi(-\xi, \xi) + \varphi(-\xi, -\xi)\Big] \\ &\qquad +C \cdot \Big[\varphi(\eta, \eta) + \varphi(\eta, -\eta) + \varphi(-\eta, \eta) + \varphi(-\eta, -\eta)\Big]. \end{aligned}$$

Now the simple integral substitution

$$z_1 = v_1 + \sqrt{T} \cdot c_1, \quad z_2 = v_2 + \sqrt{T} \cdot c_2 \tag{3.6}$$

with the constant values $\mathbf{v} = \mathbf{v}(t_n, \mathbf{x})$ and $T = T(t_n, \mathbf{x})$ enables us to compute the integral representations (3.2) by the approximate formula (3.5). The discretization in space and the interpolation of the previous fields is the same as described before.

Since we use only 12 integration knodes, this method is the fastest of the three methods that we discuss in this paper.

4 Monte Carlo calculation of the integrals

Assume that after a time step τ (relaxation time) the molecular velocities are Gaussian

$$f_n(x-\tau\mathbf{c},\mathbf{c}) = \rho_n(x-\tau\mathbf{c})\left(2\pi T_n(x-\tau\mathbf{c})\right)^{-3/2}\cdot\exp\left[-\frac{|\mathbf{c}-\mathbf{v}_n(x-\tau\mathbf{c})|^2}{2T_n(x-\tau\mathbf{c})}\right] \tag{4.1}$$

provided $\rho_n = \rho(t_n,x)$, $\mathbf{v}_n = \mathbf{v}(t_n,x)$, $T_n = T(t_n,x)$ are given. It means that $\rho_{n+1} = \rho(t_n+\tau,x)$, $v_{n+1} = v(t_n+\tau,x)$, $T_{n+1} = T(t_n+\tau,x)$ can be calculated through integral relations constructed by the conservation laws (see the relations (1.14)).

Let us suppose for simplicity that ρ, v an T do not depend on the third component of the space variable. After the explicit integration of (1.14) over the third variable we find, using the change of variables $y = x-\tau c$, that:

$$u_{n+1}(x) = \int\limits_{\mathbb{R}^2} \hat{c}_n(y)\tau^{-2}\hat{f}_n\left(y,\frac{x-y}{\tau}\right)dy. \tag{4.2}$$

Here we use the notation:

$$\mathbf{u} = \begin{pmatrix}\rho\\ \rho v_1\\ \rho v_2\\ \rho\frac{|v|^2}{2}+\frac{3}{2}\rho T\end{pmatrix}; \qquad \hat{c} = \begin{pmatrix}\rho\\ \rho c_1\\ \rho c_2\\ \rho\frac{|c|^2}{2}+\frac{1}{2}\rho T\end{pmatrix}, \tag{4.3}$$

where $c_1 = \frac{x_1-y_1}{\tau}$, $c_2 = \frac{x_2-y_2}{\tau}$, $|c|^2 = c_1^2+c_2^2$, and we set $v_3 = c_3 = 0$.

The kernel of the integral is given by

$$\hat{f}_n\left(y,\frac{x-y}{\tau}\right) = \left(2\pi T_n(y)\right)^{-1}\exp\left\{-\frac{\left|\frac{x-y}{\tau}-v_n(y)\right|^2}{2T_n(y)}\right\}. \tag{4.4}$$

Note that the integral in the form (4.4) is quite convenient in the Monte Carlo calculations. Indeed, for a fixed point x where we look for the solution, the function

$$p_n(y) = \left(2\pi\tau^2 T_n(x)\right)^{-1}\exp\left\{-\frac{|x-y-\tau v_n(x)|^2}{2\tau^2 T_n(x)}\right\} \tag{4.5}$$

is a Gaussian distribution density of y in R^2 with $x-\tau v_n(x)$ being the mean value of y, and $\tau^2 T_n(x)$ being the variance of y. If ρ, T, v are constants, then $\tau^{-2}\hat{f}_n = p_n$.

One may construct different Monte Carlo schemes for calculating the desired integrals. We will proceed as follows.

In each time step the values of the vector $\mathbf{u}_{n+1}$ are computed at the points of a uniform square grid in the unit square $[0,1]\times[0,1]$.

We introduce the following notation for the grid points:

$$\begin{aligned} x_{ij} &= ((i-1)\,h, (j-1)\,h)\,, \quad i,j = 1,\ldots,M\ , \\ h &= 1/M\ , \end{aligned}$$

and assume that $\rho_n, v_{1,n}, v_{2,n}, T_n$ are known at these points.

Sampleis a constant in the plane R^2 a random point

$$y_{ij} = x_{ij} - \tau v_n(x_{ij}) + \xi\tau\sqrt{T_n(x_{ij})}, \tag{4.6}$$

and construct the random variable (called a Monte Carlo estimator)

$$u^*_{ij} = \hat{c}_n(y_{ij})\frac{\tau^{-2}\hat{f}\left(y_{ij}, \frac{x-y_{ij}}{\tau}\right)}{p_n(y_{ij})} = \tag{4.7}$$

$$= Q\begin{pmatrix} 1 \\ (x_{ij,1}-y_{ij,1})/\tau \\ (x_{ij,2}-y_{ij,2})/\tau \\ \frac{|x_{ij}-y_{ij}|^2}{2\tau^2} + \frac{T_n(y_{ij})}{2} \end{pmatrix} = Q\begin{pmatrix} 1 \\ v_{1,n}(x_{ij}) - \xi\sqrt{T_n(x_{ij})} \\ v_{2,n}(x_{ij}) - \xi\sqrt{T_n(x_{ij})} \\ \frac{1}{2}\left(\left|v_n(x_{ij}) - \xi\sqrt{T_n(x_{ij})}\right|^2 + T_n(y_{ij})\right) \end{pmatrix}.$$

Here the weight Q is given by

$$Q = \rho_n(y_{ij})\frac{T_n(x_{ij})}{T_n(y_{ij})}\exp\left\{ -\frac{1}{2T_n(y_{ij})}\left[|v_n(x_{ij}) - v_n(y_{ij})|^2 \right.\right. \tag{4.8}$$

$$\left.\left. -2\sqrt{T_n(x_{ij})}\,\xi\cdot(v_n(x_{ij}) - v_n(y_{ij})) + |\xi|^2\,(T_n(x_{ij}) - T_n(y_{ij}))\right]\right\},$$

and ξ is a standard Gaussian random vector in R^2 with independent components that have zero means and unit variances.

Next we repeat this procedure N times and average the sum of N independent sample values of u^*_{ij}. This yields:

$$\frac{1}{N}\sum_{k=1}^{N} u_{ij}^{*(k)} \equiv \bar{u}_{ij}^{*(N)}. \tag{4.9}$$

The law of large numbers ensures that $\bar{u}_{ij}^{*(N)} \to \mathbf{u}_{n+1}(x_{ij})$ as $N \to \infty$, provided the variance of $u_{ij}^{*(k)}$ is finite.

Let us explain some technical details of the calculations. From (4.6) it follows that with probability one the value y_{ij} does not coincide with a point of the grid. Moreover, it even may fall out of the unit square where all the functions' values are considered. Thus we suppose first that in the calculations, all the functions remain undisturbed outside of the reference square, and have prescribed initial values at $t_0 = 0$. Second, to calculate the values of the functions at points y_{ij} inside the square we use a linear interpolation. This means that the simplest triangulation is imposed on the grid: every square of the grid is splitted into two triangles $(x_{ij}, u_{i+1,j}, x_{i,j+1})$ and $(u_{i+1,j+1}, x_{i+1,j}, x_{i,j+1})$.

Thus, using the values of $\rho_n, v_{1,n}, v_{2,n}, T_n$, we construct the linear interpolation for these field values at the internal points of the triangles. It is well known that the statistical error of the estimator (4.9) is of order $Var_{ij} \cdot N^{-1/2}$, where Var_{ij} is the variance of the estimator (4.7). To make it smaller, we use the properties of the u^*_{ij}-components. It is obvious, that if $\mathbf{u}_n$ is a constant, then u_{nn} has to be a constant, too. From the last term of (4.7) it follows that the Monte Carlo estimators are the desired zero-variance estimator of $\rho_{n+1}, v_{1,n+1}, v_{2,n+1}$ if we take a pair of samples

$$\xi = (\sqrt{-2\ln\alpha_1}\cos(2\pi\alpha_2),\ \sqrt{-2\ln\alpha_1}\sin(2\pi\alpha_2))$$

and $\xi' = -\xi$, since the random vector ξ is isotropic. Above, in the simulation formulas we set α_i to be independent random values uniformly distributed in $[0, 1]$. Note that the Monte Carlo estimators constructed here provide the correlated sampling of J_{ij} for different i, j. It means that for every i, j, we use the same sample values of the vector ξ. This is very

useful since it leads to dependent (consequently smooth) values of $\bar{u}_{ij}^{*(N)}$ for different i, j. This allows to evaluate smoothly the functional dependence of the computed functions on the space variable x. We note that in the problem under study, Quasi-Monte Carlo estimators seem to be useful. However, our preliminary numerical experiments with Sobol sequences do not lead to a unique conclusion about the choice what sequences or estimator are better. We mention here the following advantage of the Monte Carlo technique presented: it can be easily implemented for complicated domains in two and three dimensions. However to reach high accuracy, the convergence of the iterative procedure should be established.

5 Numerical results

In Figure 2 we compare the three integration methods developed before. As a test case, we choose initially the discontinuous mass density as $\rho_0(x_1, x_2) = 4$, if $0.4 \leq x_1, x_2 \leq 0.6$, and otherwise $\rho_0(x_1, x_2) = 1$. The velocity and temperature at the beginning are $\mathbf{v}_0(x_1, x_2) = 0, \quad T_0(x_1, x_2) = 1$.
We are interested in the fields within the space range $[0, 1] \times [0, 1]$ and within the time range $0 \leq t \leq 0.1$. In the time interval $[0, 0.1]$ we choose 30 maximizations. The Figure 2 shows the solutions for ρ, v_1, T at the final time $t = 0.1$ for $x_2 = 0.5$ and $0 \leq x_1 \leq 1$. For all three methods we use a space grid which covers $[0.1] \times [0.1]$. The mesh-wide is $dx_1 = dx_2 = 0.01$. The dotted curve results from the trapezoidal rule. At the final time $t = 0.1$ the integration domain $[-6.5, +6.5] \times [-6.5, +6.5]$ is decomposed into 50 subintervals in each direction.
The solid curve represents the Gaussian integration formula of degree 7, while the dashed curve represents the results of the Monte Carlo method with $N = 10.000$ Monte Carlo points.
Figure 3 illustrates the global solution at time $t = 0.1$. The light and dark colours correspond to small and large values of the fields, respectively, ranging from $\rho_{min} = 1.0$, $v_{1,min} = -0.5$, $T_{min} = 0.6$ (light color) to $\rho_{max} = 4.0$, $v_{1,max} = 0.5$, $T_{max} = 1.25$ (black color).

Finally we consider the interaction of two spherically symmetric fields

which evolve from the following initial data:

$$\rho_0(x_1, x_2) = 4 \text{ for } (x_1 - 0.4)^2 + (x_2 - 0.4)^2 \leq 0.015$$

and for $(x_1 - 0.6)^2 + (x_2 - 0.6)^2 \leq 0.015$. Otherwise $\rho(x_1, x_2) = 1$, and $v_1 = v_2 = 0, T = 1$.

The Figure 4 shows the resulting fields of mass density, of the x_1-component of the velocity and of the temperature at time $t = 0.15$. As before, the light and dark colours correspond to small and large values of the fields, respectively, ranging from $\rho_{min} = 1.0$, $v_{1,min} = -0.6$, $T_{min} = 0.6$ (light color) to $\rho_{max} = 4.0$, $v_{1,max} = 0.6$, $T_{max} = 1.4$ (black color). The Gaussian integration rule is used for the results which are displayed in Figure 3 and Figure 4.

6 Conclusions

A numerical iteration procedure is suggested to find the approximate solution of the Euler equations in two and three dimensions. In each step of the iterative scheme, we evaluate multidimensional integrals over the velocity field. Three approximate integration methods were used: the trapezoidal rule, the Gaussian formulae, and a Monte Carlo dependent sampling technique. The numerical results obtained by these methods show a good agreement in the 2D case. The Monte Carlo results were also obtained for a 3D cube with similar data as used in 2D case. However, from the construction of the iterative scheme it is clear that the Monte Carlo method presented here can be easily applied to domains with complicated geometry. To guarantee a high accuracy, the convergence and stability of the iterative scheme should be established.

References

[1] G. Boillat, T. Ruggeri. Moment equations in the kinetic theory of gases and wave velocities. *Cont. Mech. Thermodyn.*, **9** (1997), N 4.

[2] W. Dreyer. Maximization of the Entropy in Non-Equilibrium. *J. Phys. A.: Math. Gen*, **20** (1987).

[3] W. Dreyer, M. Kunik. The Maximum Entropy Principle Revisited. *WIAS-Preprint* No. 367 (1997), Cont. Mech. Thermodyn. **11**, N 1, in press.

[4] W. Dreyer, M. Kunik. Reflections of Eulerian shock waves at moving adiabatic boundaries. *Monte Carlo Methods and Applications*, **4** (1998), N3, 231-252.

[5] C. D. Levermore. Moment Closure Hierarchies for Kinetic Theories. *J. Stat. Phys.* **83** (1996), 1021–1065.

[6] I. Müller, T. Ruggeri. Extended Thermodynamics. Springer Verlag, New York, 1993.

[7] B. Pertame. The kinetic approach to systems of conservation laws. In: *Recent advances in partial differential equations.* Editors M.A. Herrero and E. Zuazua, Wiley and Mason (1994), 85-97.

[8] A.H. Stroud, D. Secrest. Approximate Integration Formulas for certain Spherical Symmetric Region. *Math. Comp.* **17** (1963), 105-135.

Fig. 2 Three different integration methods:

Trapezoidal (pointed), Gaussian (solid) and Monte Carlo (dashed)

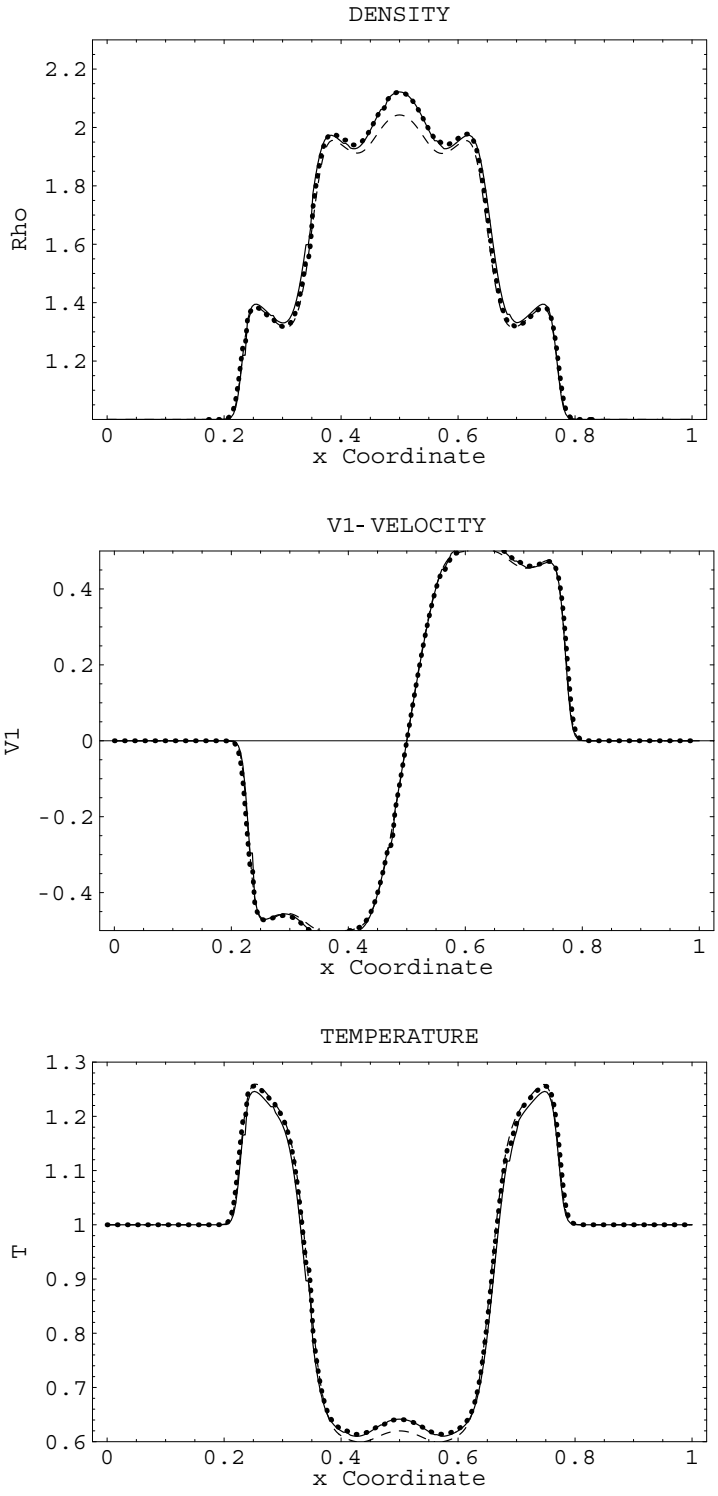

Fig. 3 The global solution for the quadratic pulse

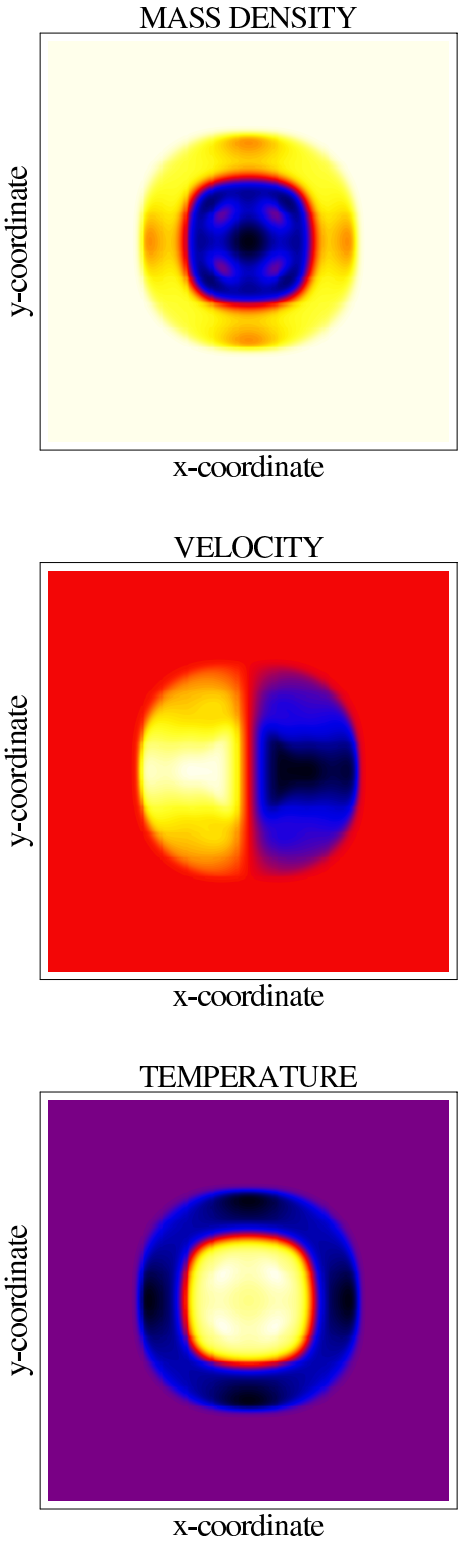

Fig. 4 Two interacting spherically waves